

Effects of Non-nucleonic Degrees of Freedom in the $D(\vec{p}, \gamma)^3\text{He}$ and $p(\vec{d}, \gamma)^3\text{He}$ Reactions

G. J. Schmid,^{1,2,*} M. Viviani,³ B. J. Rice,^{1,2} R. M. Chasteler,^{1,2} M. A. Godwin,^{1,2} G. C. Kiang,⁴ L. L. Kiang,⁵
A. Kievsky,³ C. M. Laymon,^{1,2} R. M. Prior,⁶ R. Schiavilla,^{7,8} D. R. Tilley,^{2,9} and H. R. Weller^{1,2}

¹*Department of Physics, Duke University, Durham, North Carolina 27708*

²*Triangle Universities Nuclear Laboratory, Duke Station, Durham, North Carolina 27708*

³*INFN, Sezione di Pisa, 56100 Pisa, Italy*

⁴*Academia Sinica, Taipei, Taiwan*

⁵*National Tsing-Hua University, Taipei, Taiwan*

⁶*Department of Physics, North Georgia College, Dahlonega, Georgia 30597*

¹*CEBAF Theory Group, Newport News, Virginia 23606*

⁸*Department of Physics, Old Dominion University, Norfolk, Virginia 23529*

⁹*Department of Physics, North Carolina State University, Raleigh, North Carolina 27695*

(Received 15 November 1995)

Measurements of the $D(\vec{p}, \gamma)^3\text{He}$ and $p(\vec{d}, \gamma)^3\text{He}$ reactions below $E_{p,d} = 80$ keV are compared to the results of calculations based on correlated hyperspherical harmonic wave functions obtained from realistic interactions with full inclusion of Coulomb distortion in the initial continuum state, and a nuclear current operator with one- and two-body components. Dramatic effects due to the tensor force and the associated two-body (meson-exchange) interaction currents are observed in the vector and, to some extent, tensor analyzing powers for the first time. The extrapolation to zero energy leads to an S -factor value of $S(E=0) = 0.165 \pm 0.014$ eV b, in reasonable agreement with theory. [S0031-9007(96)00008-7]

PACS numbers: 25.40.Lw, 21.45.+v, 24.70.+s, 27.10.+h

Weak and radiative capture reactions on few-nucleon systems at very low energies have great astrophysical importance in relation to studies of stellar structure and evolution [1]. Two such aspects are as follows: (1) the mechanism for the energy and neutrino production in main sequence stars, in particular, the determination of the solar neutrino flux; and (2) the process of protostellar evolution toward the main sequence. A quantity of interest in the latter area is the zero-energy astrophysical S factor for $D(p, \gamma)^3\text{He}$, whose currently accepted value was first determined over 30 years ago by extrapolating low energy cross-section data using a direct capture model [2].

Besides their astrophysical relevance, these reactions are very interesting from the aspect of the many-body theory of strongly interacting systems since they are sensitive to ground- and scattering-state wave functions and the full nuclear electroweak transition operators. Indeed, calculations of the $D(n, \gamma)^3\text{H}$ and $^3\text{He}(n, \gamma)^4\text{He}$ capture cross sections at thermal neutron energies carried out with realistic wave functions and a single-nucleon electromagnetic current, the so-called impulse approximation (IA), predict only about 50% [3,4] and 10% [5] of the corresponding empirical values. This is because the IA transition operator cannot connect the main S -state components of the deuteron and ^3H , or ^3He and ^4He , wave functions. Hence, the calculated cross section in IA is small since the reaction must proceed through the small components of the wave functions. Two-body currents, however, can connect the dominant S -state components, and the associated matrix elements are exceptionally large in comparison to those obtained in IA [3–5].

The data of this paper, some of which were reported recently [6], were obtained using a polarized proton beam at 80 keV in a study of the $D(\vec{p}, \gamma)^3\text{He}$ reaction, along with a tensor-polarized deuteron beam at 80 keV to measure the tensor analyzing power $T_{20}(\theta)$ for the $p(\vec{d}, \gamma)^3\text{He}$ reaction. The polarized beams were produced by the Triangle Universities Nuclear Laboratory (TUNL) atomic beam polarized ion source, with typical beam currents of 30 mA on target. Fast spin flip (10 Hz) was employed for both measurements. In the case of the vector analyzing power $A_y(\theta)$ measurements, the two vector-polarized spin states had their axes of symmetry aligned perpendicular to the reaction plane. In the case of the $T_{20}(\theta)$ measurements, the spin-symmetry axis was aligned along the beam axis ($\beta = 0$), thus eliminating other beam moments, and the beam was switched between states having $p_{zz} = +0.84 \pm 0.02$ and -0.86 ± 0.02 . Beam polarizations were measured by charge-exchanging these positive-ion beams, then accelerating them through the TUNL tandem, where standard ^{12}C and ^3He polarimeters were used. The deuteron beam polarization was monitored at frequent intervals during the experiment via the $D(d, n)^3\text{He}$ reaction at 80 keV, using a deuterated titanium target in a polarimeter located in the low energy beam line. The targets were frozen D_2O and frozen H_2O samples, respectively, which were thick enough to stop the 80 keV beams in both cases.

The outgoing γ rays were detected in a large volume (130% efficient) high-purity germanium (HPGe) detector, surrounded by a 5 cm thick NaI annulus, which was run in the anticoincidence mode. The high resolution of the HPGe detector (4.2 keV at 5.5 MeV) made it possible to

extract the energy dependence of the cross section and analyzing power from the full detector response function after removing the intrinsic detector response function and the energy-dependent target thickness effects. Details of the deconvolution procedure used to perform this are described in Ref. [6]. This procedure produced the result shown in Fig. 1 for the magnitude and slope of the S factor. In addition to the deconvolution procedure, the data from the $D(p,\gamma)^3\text{He}$ reaction were also analyzed by binning the full response function of the detector into 10 keV bins [6]. The results of this procedure are also shown in Fig. 1. Although these results do not determine the S factor at $E = 0$ as precisely as the deconvolution method, it is reassuring to see that the two methods are consistent.

The experimental data points and curve presented in Fig. 1 are equivalent to the results presented in Ref. [6], with the exception that the absolute scale has been altered. An overall scaling factor of 1.37 has been applied to correct for an error in the values for the detector efficiency used in Ref. [6]. This error was due to a systematic error in Ref. [7] in the relative intensities for the lines in ^{66}Ga which were used to extrapolate our measured efficiencies up to 5.5 MeV. By applying the appropriate correction factors [8] to the results of Ref. [7], we obtain an efficiency value at 5.5 MeV which is in excellent agreement with the results of both a recent Monte Carlo calculation and an independent calibration measurement using the $^{19}\text{F}(p,\alpha\gamma)$ reaction [9]. Complete details of all the procedures which relate to the new efficiency are forthcoming [10]. However, we quote here the updated value for the S factor at zero energy: $S(0) = 0.165 \pm 0.014$ eV b (including both statistical and systematic errors), which is 34% lower than the result of Ref. [2].

The binned data were also used to obtain the vector analyzing powers as a function of energy. Although this

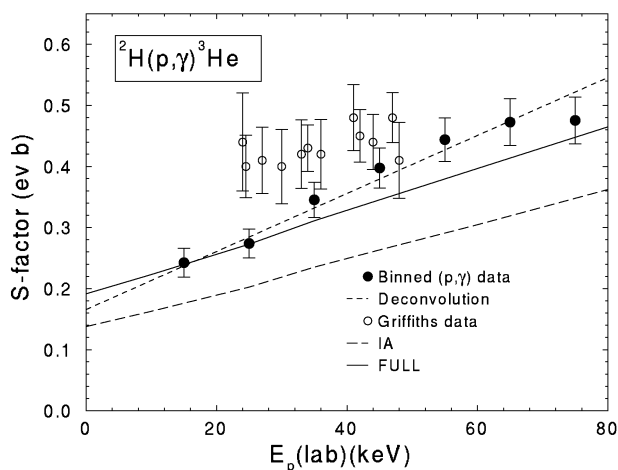


FIG. 1. A comparison between experimental values and results of variational calculations for the S factor of $D(p, \gamma)^3\text{He}$ with $E_p(\text{lab}) = 80\text{--}0$ keV. Note that the experimental results presented here differ from those presented in Ref. [6] by an overall scaling factor of 1.37 (see text).

procedure allowed us to obtain $A_y(\theta)$ as a function of energy, the statistical errors on the low energy points are substantial. This fact, coupled with our observation of very little energy dependence, has led us to present the full energy integrated data in this paper. Accordingly, we have integrated the theoretical calculations, weighted by the energy dependence of the cross section and the target thickness, for the purpose of comparing them with the data.

The NaI annulus which surrounded the HPGe detector was actually a quadrated annulus oriented such that two segments were in the reaction plane, and two were perpendicular to it. This setup allowed us to measure the linear polarization of the γ rays from the $D(p,\gamma)^3\text{He}$ reaction by observing the Compton scattered events in the four segments. In addition to a coincidence requirement, our software was constructed to require that the summed energy observed in the HPGe detector plus the NaI segment equaled the full energy of the capture γ ray. This γ -ray “polarimeter” was calibrated using the 4.4 MeV γ rays from the $^{12}\text{C}(p, p'\gamma)^{12}\text{C}$ reaction, and the 1.78 MeV γ rays from the $^{28}\text{Si}(p, p'\gamma)^{28}\text{Si}$ reaction. These two points were used to extrapolate the polarization sensitivity of this polarimeter to 5.5 MeV, using the functional form obtained from the Klein-Nishina formula (in the point detector approximation), and fitting it to the two measured points. The results indicated a polarization sensitivity of $(3.5 \pm 0.35)\%$ for the 5.5 MeV γ rays of the present experiment. A full presentation of the γ -ray polarization measurements for $D(p,\gamma)^3\text{He}$ will be included in a future publication [11].

Friar and collaborators have recently calculated the S -wave contribution to the S factor of the $D(p,\gamma)^3\text{He}$ reaction at zero energy [12]. The calculations were based on converged bound- and scattering-state Faddeev wave functions obtained from a realistic Hamiltonian, including the Coulomb interaction, and a nuclear current operator in which the two-body part was constrained by reproducing the measured $D(n,\gamma)^3\text{He}$ total cross section at thermal neutron energies. The predicted value for $S_S(E = 0)$ is 0.108 eV b [12], in excellent agreement with the $M1$ S factor extracted from the present data: $S_S(E = 0) = 0.109 \pm 0.010$ eV b. The present data also yield a value for the $E1$ S factor: $S_P(E = 0) = 0.73 \pm 0.007$ eV b.

An extended account of the calculations carried out in the present Letter will be published elsewhere [4]. Here, we briefly describe the correlated hyperspherical harmonics (CHH) method used to generate the bound- and scattering-state wave functions, and the general structure of the nuclear current operator.

The CHH wave function of the trinucleon bound state is written as [13]

$$\psi_3 = \sum_{\alpha=1}^{N_c} \sum_{K=K_0}^{K_M} \frac{u_{\alpha K}(\rho)}{\rho^{5/2}} \times \sum_{ijk \text{ cyclic}} f_{\alpha}(r_{jk}) {}^{(2)}P_K(\phi_i) Y_{\alpha}(jk, i), \quad (1)$$

where ρ is the hyperradius, $\rho = \sqrt{x_i^2 + y_i^2}$ with $\mathbf{x}_i = \mathbf{r}_j - \mathbf{r}_k$ and $\mathbf{y}_i = (\mathbf{r}_j + \mathbf{r}_k - 2\mathbf{r}_i)/\sqrt{3}$, \mathbf{r}_i denoting the position of particle i , and $\cos\phi_i = x_i/\rho$. Explicit expressions for the angular spin-isospin functions $Y_\alpha(jk, i)$ and hyperangular polynomials ${}^{(2)}P_K(\phi_i)$ as well as a discussion of the method used to determine the state-dependent correlation functions $f_\alpha(r_{jk})$ can be found in Ref. [13]. Here we only note that the label α specifies a given combination of orbital angular momenta and spin-isospin

$$\psi_{2+1}^{JJ_zLS} = \psi_c + \sum_{ijk \text{ cyclic}} \sum_{L'S'} \{[\phi_d(\mathbf{x}_i) \otimes s^i]_{S'} \otimes Y_{L'}(\hat{\mathbf{y}}_i)\}_{JJ_z} \left[\delta_{LL'} \delta_{SS'} \frac{F_L(pr_{dp})}{pr_{dp}} + {}^J R_{LS}^{L'S'} \frac{G_L(pr_{dp})}{pr_{dp}} g(r_{dp}) \right], \quad (2)$$

where ϕ_d is the deuteron wave function, r_{dp} and p are the distance and relative momentum between deuteron and proton, respectively, and $F_L(G_L)$ is the regular (irregular) Coulomb function. The function $g(r_{dp})$ modifies the $G_L(pr_{dp})$ at small r_{dp} by regularizing it at the origin, and is one for $r_{dp} \geq 10$ fm, thus not affecting the asymptotic behavior of $\psi_{2+1}^{JJ_zLS}$. The sum over $L'S'$ is over all values compatible with a given J and parity. The internal wave function ψ_c describes the system when the nucleons are close to each other, and is parametrized as the bound-state wave function described above. The R -matrix elements ${}^J R_{LS}^{L'S'}$ and the $u_{\alpha K}(\rho)$ in ψ_c are determined variationally by minimizing the functional [14]

$$[{}^J R_{LS}^{L'S'}] = {}^J R_{LS}^{L'S'} - \langle \psi_{2+1}^{JJ_zLS} | H - E_d - \frac{3}{4m} p^2 | \psi_{2+1}^{JJ_zLS} \rangle \quad (3)$$

with respect to variations in the ${}^J R_{LS}^{L'S'}$ and $u_{\alpha K}$. Here $E_d = -2.225$ MeV is the deuteron binding energy. As in the bound state problem, the hyperradial functions $u_{\alpha K}(\rho)$ are required to vanish in the limit of large ρ .

The Hamiltonian used in the present calculations consists of the Argonne v_{18} two-nucleon [15] and Urbana model-IX three-nucleon [16] interactions. The ${}^3\text{H}$ and ${}^3\text{He}$ binding energies obtained with the CHH wave functions reproduce the corresponding empirical values. The calculated $d + n$ ($d + p$) doublet and quartet scattering lengths are 0.63(−0.02) and 6.33(13.7) fm [17], respectively. The $d + n$ doublet and quartet scattering lengths above are to be compared with the empirical values 0.65 ± 0.04 and 6.35 ± 0.02 fm [18], respectively. It should also be stressed that predictions based on CHH wave functions for a variety of properties depending on both ground and low-energy continuum states of the trinucleons are in excellent agreement with the corresponding Faddeev results [19].

The transition amplitude between an initial $d + p$ continuum state with deuteron and proton spin projections σ_2 and σ , respectively, and relative momentum \mathbf{p} , and a final ${}^3\text{He}$ state with spin projection σ_3 is given by

$$j_{\sigma_3 \sigma_2 \sigma}^\alpha(\mathbf{p}, \mathbf{q}) = \langle \psi_{\sigma_3} | \epsilon_\alpha \int d\mathbf{x} e^{-i\mathbf{q}\cdot\mathbf{x}} \mathbf{j}(\mathbf{x}) | \psi_{\mathbf{p}, \sigma_2 \sigma}^{(+)} \rangle, \quad (4)$$

states, and that the $Y_\alpha(jk, i)$ are odd under the interchange $j \leftrightarrow k$ in order to ensure the antisymmetry of the wave function. The Rayleigh-Ritz variational principle is used to determine the hyperradial functions $u_{\alpha K}(\rho)$ by minimizing a Hamiltonian including nonrelativistic kinetic energies and realistic two- and three-nucleon interactions [13].

The $d + p$ scattering state wave function is written as [14]

where ϵ_α is the polarization of the photon and $\mathbf{j}(\mathbf{x})$ is the nuclear current density. The partial wave expansion of the wave function $\psi^{(+)}$ (with outgoing wave boundary condition) in terms of the $\psi_{2+1}^{JJ_zLS}$ introduced above is well known, and will not be given here. Expressions for the cross section, vector and tensor analyzing powers, and photon linear polarization are easily obtained from the amplitudes $j_{\sigma_3 \sigma_2 \sigma}^\alpha$ [4]. The measured angular distributions of these observables (Fig. 2) indicate that the reaction proceeds through S - and P -wave capture. The S - (P -) wave capture is dominated by $M1$ ($E1$) radiation, while contributions due to $E2$ ($M2$) transitions have been found to be negligible in the energy range under consideration [4].

The nuclear current density operator consists of one- and two-body parts. The former has the standard expression in terms of single-nucleon convection and spin-magnetization

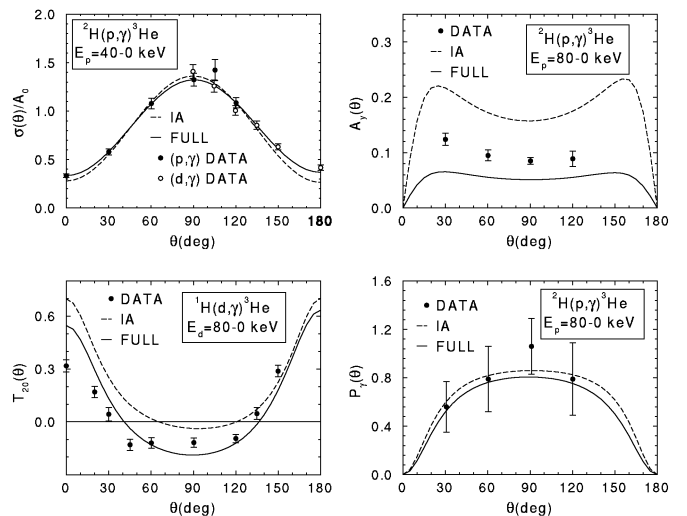


FIG. 2. A comparison between experimental values and results of variational calculations for $\sigma(\theta)$, $A_y(\theta)$, and $P_\gamma(\theta)$ for the $D(p,\gamma){}^3\text{He}$ reaction, and $\sigma(\theta)$ and $T_{20}(\theta)$ for the $p(d,\gamma){}^3\text{He}$ reaction. In each plot, the solid curve corresponds to the results obtained with one- and two-body currents, while the dashed curve is obtained in the impulse approximation. Note that the $\sigma(\theta)$ plot shows (p,γ) data with $E_p = 40-0$ keV ($E_{c.m.} = 27-0$ keV) instead of $80-0$ keV. This is done to allow the (d,γ) data with $E_d = 80-0$ keV ($E_{c.m.} = 27-0$ keV) and the (p,γ) data to be shown in the same graph [with the (d,γ) data plotted using (p,γ) angles $\theta_p = 180^\circ - \theta_d$].

currents, while explicit expressions for the latter can be found in Refs. [5,20,21]. Two aspects of the two-body current model used in the present calculations should be emphasized. First, their dominant isovector terms are constructed from the tensor components of the two-nucleon interaction [15], following a prescription originally proposed by Riska [22]. Additional, but far less important, two-body currents of both isoscalar and isovector character are obtained by minimal substitution in the momentum-dependent terms of the interaction [5,20]. While the Riska prescription is not unique, it does generate two-body currents that satisfy current conservation exactly. Furthermore, it has been shown to provide, at low and moderate values of momentum transfers (≤ 1 GeV/c), a satisfactory description of the deuteron threshold electrodisintegration [23], $^1\text{H}(n,\gamma)^2\text{H}$ capture cross section at thermal neutron energies [23], and magnetic moments and form factors of the trinucleons [20,24]. Second, as discussed in Ref. [21], Δ -isobar degrees of freedom are explicitly included in the nuclear wave functions rather than being eliminated in favor of effective two-body operators acting on the nucleons' coordinates. The latter perturbative treatment has been shown to be inaccurate, particularly in reactions as delicate as the $^3\text{He}(n,\gamma)^4\text{He}$ capture at thermal neutron energies [21]. For the present reaction, however, it leads only to an $\approx 8\%$ overestimate of the doublet $M1$ reduced matrix element when compared to the result obtained with the more accurate nonperturbative treatment [4].

The S factor calculated with and without inclusion of two-body currents is compared with that obtained in the present experiment in Fig. 1. Also shown in Fig. 1 are the previous data of Griffiths *et al.* [2]. Both the absolute values and energy dependence of the present data are well reproduced by the full calculation. The enhancement due to two-body current contributions is substantial: the ratios $[S(\text{full}) - S(\text{IA})]/S(\text{IA})$ for the S - and P -wave S factors are found to be, respectively, 0.62 and 0.18 at 0 keV, and increase to 0.71 and 0.20 at 80 keV. In particular $S_S(E=0) = 0.105$ eV b, close to the value 0.108 eV b obtained by Friar *et al.* [12], and in good agreement with the present experimental determination: $S_S(E=0) = 0.109 \pm 0.010$ eV b.

The predicted angular distributions of the relative cross section, vector and tensor analyzing powers, and photon linear polarization are compared with data in Fig. 2. The overall agreement between theory and experiment is satisfactory for all observables with the exception of $A_y(\theta)$. This latter observable is particularly sensitive to two-body current contributions: their effect is to reduce the results obtained in IA by about a factor of 3, bringing them into better agreement with the data. However, a $\approx 30\%$ discrepancy between theory and experiment remains unresolved. It is important to recall here that these observables, unlike thermal cross sections, are independent of normalization issues in both theory and experiment.

In summary, cross sections and polarization observables for the $D(\vec{p}, \gamma)^3\text{He}$ and $p(\vec{d}, \gamma)^3\text{He}$ capture reactions have

been measured in the energy range 0–80 keV for the first time. *Ab initio* microscopic calculations based on CHH wave functions obtained from realistic interactions and a current operator including one- and two-body components provide a satisfactory description of all measurements, including the S factor, with the exception of the vector analyzing power data, which are substantially underestimated by theory, but which are seen to be particularly sensitive to two-body current contributions. The observed discrepancy between the predicted and measured $A_y(\theta)$ suggests that further refinements of our present treatment of these effects, such as the inclusion of three-body currents associated with the three-nucleon interaction, are required. Such studies are being vigorously pursued.

Most of the calculations reported here were made possible by a grant of time on the Cray supercomputers at the NERSC, Livermore, California. This work was supported in part by the U.S. DOE under Contract No. DEFG05-91-ER40619.

*Present address: Lawrence Berkeley National Laboratory, University of California, Berkeley, California 94720.

- [1] C. E. Rolfs and W. S. Rodney, *Cauldrons in the Cosmos* (University of Chicago Press, Chicago, 1988).
- [2] G. M. Griffiths, M. Lal, and C. D. Scarfe, *Can. J. Phys.* **41**, 724 (1963).
- [3] J. L. Friar, B. F. Gibson, and G. L. Payne, *Phys. Lett.* **251B**, 11 (1990).
- [4] M. Viviani, A. Kievsky, and R. Schiavilla (to be published).
- [5] J. Carlson *et al.*, *Phys. Rev. C* **42**, 830 (1990).
- [6] G. J. Schmid *et al.*, *Phys. Rev. C* **52**, R1732 (1995).
- [7] C. Alderliesten *et al.*, *Nucl. Instrum. Methods* **A335**, 219 (1993).
- [8] G. J. McCallum and G. E. Coote, *Nucl. Instrum. Methods* **124**, 309 (1975).
- [9] L. Ma *et al.* (private communication).
- [10] G. J. Schmid *et al.* (to be published).
- [11] G. J. Schmid *et al.* (to be published).
- [12] J. L. Friar *et al.*, *Phys. Rev. Lett.* **66**, 1827 (1991).
- [13] A. Kievsky, M. Viviani, and S. Rosati, *Nucl. Phys.* **A551**, 241 (1993).
- [14] A. Kievsky, M. Viviani, and S. Rosati, *Nucl. Phys.* **A577**, 511 (1994).
- [15] R. B. Wiringa, V. G. J. Stoks, and R. Schiavilla, *Phys. Rev. C* **51**, 38 (1995).
- [16] B. S. Pudliner *et al.*, *Phys. Rev. Lett.* **74**, 4396 (1995).
- [17] A. Kievsky, M. Viviani, and S. Rosati, *Phys. Rev. C* **52**, R15 (1995).
- [18] W. Dilg, L. Koester, and W. Nistler, *Phys. Lett.* **36B**, 208 (1971).
- [19] D. Hüber *et al.*, *Phys. Rev. C* **51**, 1100 (1995).
- [20] R. Schiavilla, V. R. Pandharipande, and D. O. Riska, *Phys. Rev. C* **40**, 2294 (1989).
- [21] R. Schiavilla *et al.*, *Phys. Rev. C* **45**, 2628 (1992).
- [22] D. O. Riska, *Phys. Scripta* **31**, 471 (1985).
- [23] R. Schiavilla and D. O. Riska, *Phys. Rev. C* **43**, 437 (1991).
- [24] R. B. Wiringa, *Phys. Rev. C* **43**, 1585 (1991).